GSA Data Repository 2017361

Wolff, 2017, On the syenite-trachyte problem: Geology, doi:10.1130/G39415.1

Construction of Fig. 1A:

Files for "Trachytes" and "Phonolites" were downloaded from GEOROC <georoc.mpch-mainz.gwdg.de> in the period April - July 2016. The following filters were applied to the data:

1. Sufficiently complete major-element analyses to enable calculation of the CIPW norm.
2. Raw totals in the range 95% – 101.5%. The low limit was set because glassy felsic volcanic rocks frequently have water of hydration that may not greatly affect the major and minor oxides; see also condition 5 below.
3. Differentiation index (normative $Q + or + ab + lc + ne + ns$) ≥ 75%.
4. The following CIPW norm-based definitions of phonolite, trachyte and quartz trachyte were applied: phonolite, ≥ 10% *ne*; trachyte, < 10% *ne*, < 10% *Q*; high-quartz trachyte, ≥ 10% *Q*. These definitions resulted in many analyses being shifted between the phonolite and trachyte categories of the GEOROC classification. Here, high-quartz trachytes are rocks with >10% normative *Q* and < 69% SiO_2; the term is used because "quartz trachyte" has historically been applied to any trachyte with normative quartz. No rhyolites are plotted in Fig. 1A.
5. No normative corundum. In my experience, most cases of normative *C* in analyses of alkaline volcanic rocks, especially glassy rocks, are due to alkali removal by weathering, even for cases where the analytical total exceeds 95%. Some examples of truly *C*-normative rocks may have been lost from the database by adopting this procedure.
6. Inspection and removal of clearly non-magmatic compositions. These amounted to <<1% of the total number of analyses.

A total of 4413 analyses passed the filters. These analyses were recalculated to $Fe^{2+}/Fe_{tot} = 0.7$ indicated by trial rhyolite-MELTS (Ghiorso and Sack, 1994; Gualda et al., 2012) calculations at oxygen fugacities corresponding to the NNO buffer. This $f(O_2)$ assumption may be incorrect in many cases; however the effect on the norm and the position of the sample in *Q* - *ne* - *ks* (Fig. 1A) is small due to condition 3 above.

Crystallization of felsic alkaline magmas

It is obvious from the normative compositions of the rocks plotted in Fig. 1 that alkali feldspar must be the dominant phase crystallizing from the liquids. This is well illustrated by experiments on natural samples. An example is shown in Fig. DR1, from the experimental study of Andújar et al. (2008). The bulk composition lies on the feldspar surface in Figs. 1 and 2, but close to the phonolite minimum, and may therefore be regarded as a 'least favorable' case. Although mafic phases are the first to crystallize, their total abundance never rises above 6%. Crystallinities

approaching the rheological threshold (>30%) are only achieved after alkali feldspar joins the crystallizing assemblage and then dominates (>85% of the assemblage) as temperature falls (Fig. DR1). Although a feldspathoid (haüyne) formed in these experiments, it is only present in trace amounts (Andújar et al., 2008). Hence, the cumulate formed by mechanical separation of this assemblage will be syenitic (*sensu stricto*).

Calculation of viscosities, densities and settling rates

Viscosities and densities as a function of water content at 100 MPa and two temperatures (750 and 850 °C) for melts with the compositions of the twelve phonolites and trachytes in Table DR1 are shown in Figs. DR2 and DR3. Viscosities were calculated using the procedure of Giordano et al. (2008); silicate melt densities were calculated using the method and data of Lange and Carmichael (1987, 1990), Kress and Carmichael (1991), and Ochs and Lange (1999). Densities of solid phases under the same conditions were calculated using the MELTS supplemental calculator (Ghiorso and Sack, 1994) except for sodalite (data from Sharp et al., 1989).

Settling times for feldspar crystals of different sizes in the silicate melts given in table DR1 for the same range of conditions were calculated using the hindered settling model of Bachmann and Bergantz (2004: their eqns. 2–4):

$$U_{\mathrm{hs}} = U_{\mathrm{Stokes}} . f(c)$$

where U_{hs} is the hindered settling velocity and U_{Stokes} is the Stokes settling velocity:

$$U_{\mathrm{Stokes}} = 2r^2 g \Delta\rho / 9\mu$$

(in which r = particle radius, g is acceleration due to gravity, ρ and μ are melt density and dynamic viscosity respectively), modifed by factor $f(c)$, a correction for crystal fraction c (Barnea and Mizrahi, 1973):

$$f(c) = (1 - c)^2 / (1 + c^{1/3})^{[5c/3(1 - c)]}$$

The time to clarify 500 m thickness of magma by hindered settling of feldspar crystals, corresponding to the range c = 0.3 – 0.6, for two cases is shown in Fig. DR4. The calculation was performed stepwise with a new value of $f(c)$ calculated for each 0.005 increase in c. The two cases in Fig. DR4 are extremes; all other compositions in Table DR1 give results that fall between the two cases plotted over the range of conditions used.

Data repository table

	1	2	3	4	5	6	7	8	9	10	11	12
SiO_2	56.36	60.27	58.67	59.82	65.61	63.65	61.01	62.81	69.06	62.67	61.50	61.07
TiO_2	0.51	0.66	0.44	0.88	0.37	0.72	1.05	0.57	0.20	0.75	0.45	0.41
Al_2O_3	21.55	19.24	20.05	19.50	16.69	18.44	19.47	12.98	15.72	17.19	18.65	18.48
FeO*	2.54	2.92	2.44	2.96	3.39	3.11	3.97	9.03	1.56	4.05	3.17	3.41
MnO	0.17	0.23	0.19	0.15	0.26	0.15	0.15	0.34	0.21	0.19	0.23	0.10
MgO	0.74	0.25	0.40	0.59	0.16	0.49	0.98	0.21	0.18	0.96	0.40	0.76
CaO	1.78	0.64	2.05	2.30	0.68	1.30	2.14	1.08	0.90	3.22	1.90	2.53
Na_2O	10.97	10.14	9.79	8.12	7.20	5.66	5.26	8.27	6.85	6.59	6.11	3.02
K_2O	5.30	5.58	5.92	5.56	5.62	6.35	5.77	4.64	5.28	4.09	7.55	10.08
P_2O_5	0.07	0.06	0.05	0.13	0.03	0.14	0.20	0.06	0.03	0.29	0.05	0.15

Table DR1. Compositions, normalized to 100% volatile-free, of natural phonolites and trachytes used in viscosity and density calculations. 1–4, Tenerife phonolites: 1 = TF01-88, 2 = 01TF85N, 3 = TF00-62, 4 = TF0039 (Edgar et al., 2002; Olin, 2007; Andújar et al., 2008). 5–7, Fogo A trachyte, São Miguel: 5 = ASM220, 6 = ASM216, 7 = ASM217 (Widom et al., 1992). 8 = Longonot Fe-rich quartz trachyte 29Lt2 (Rogers et al., 2004). 9, 10, Massif Central quartz trachytes: 9 = CHO, 10 = CLI (Martel et al., 2013). 11, 12, Campanian Ignimbrite silica-undersaturated trachytic glasses: 11 = average of VOS1 glass, 12 = average of PRO2 glass (Forni et al., 2016).

Data Repository Figures

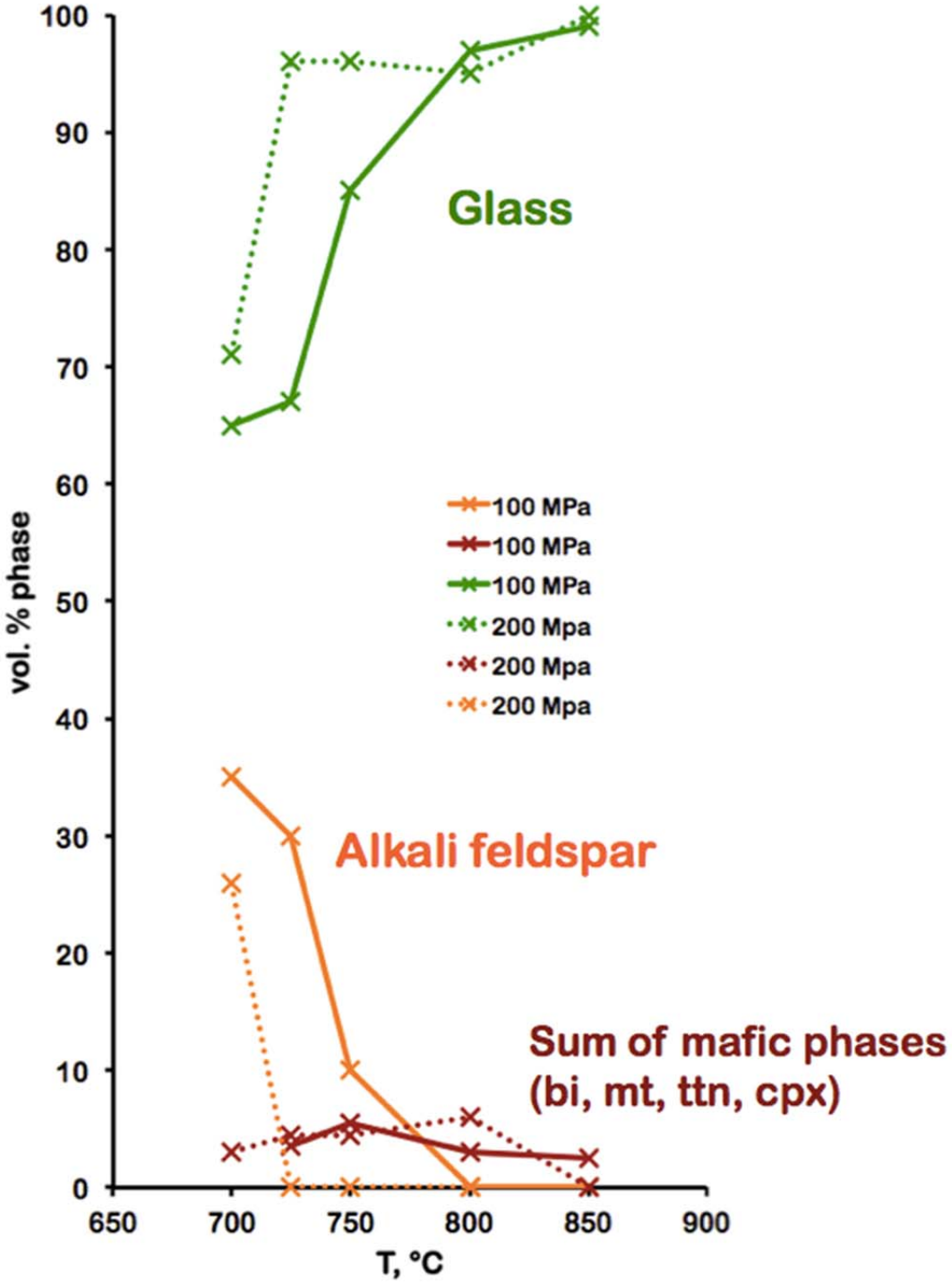

Figure DR1. Phase abundances in fluid-saturated experiments of Andújar et al. (2008) on Tenerife phonolite 01TF85N (Table DR1), at 100 and 200 MPa, in the range 700 – 850 °C. bi = biotite, mt = magnetite, ttn = titanite, cpx = clinopyroxene.

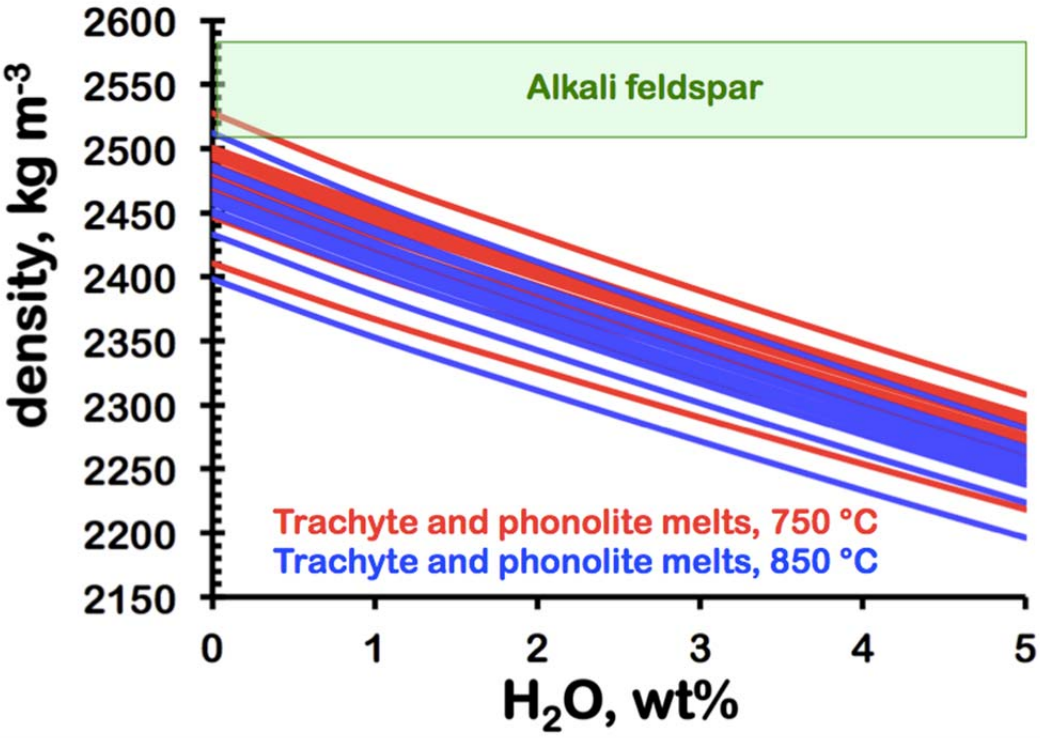

Figure DR2. Densities of phonolite to quartz trachyte melts listed in Table DR1 as a function of water content, and alkali feldspar, at 100 MPa and two different temperatures. Feldspar compositions represented by the green box are $An_{15}Ab_{70}Or_{15}$, $Ab_{80}Or_{20}$, $Ab_{50}Or_{50}$, and $Ab_{20}Or_{80}$, thus covering the range from ternary-composition anorthoclase to potassic sanidine expected to crystallize from a variety of sodic to potassic trachytes and phonolites.

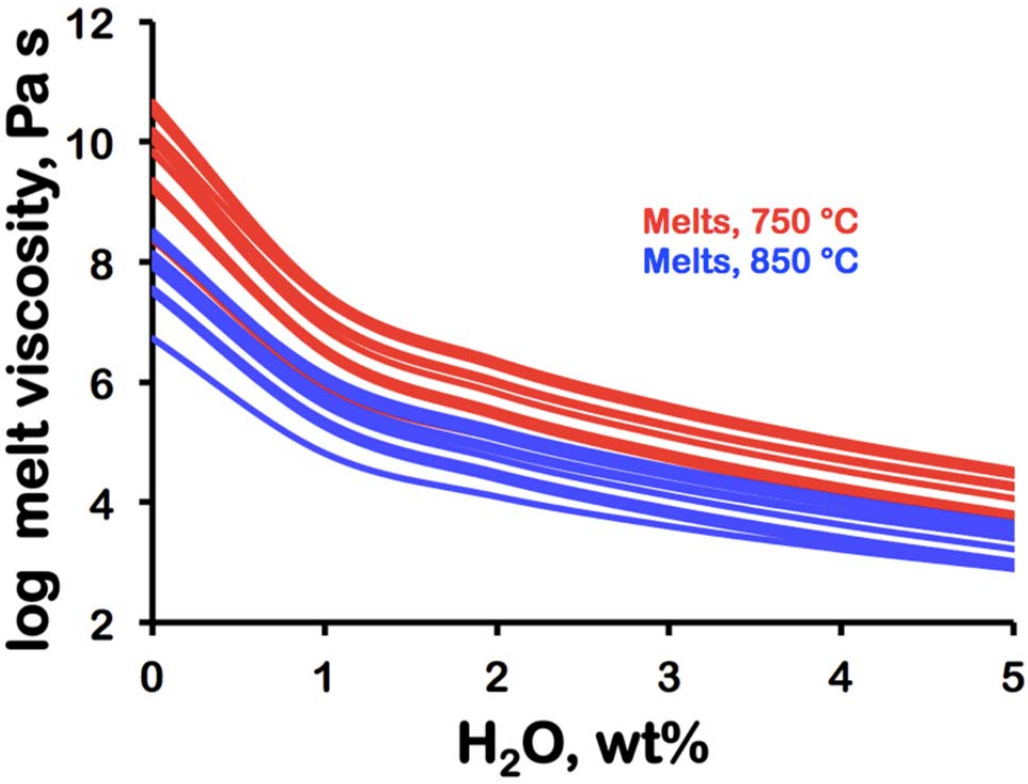

Figure DR3. Viscosities of phonolite to quartz trachyte melts, calculated for the same conditions as melt densities in Fig. DR2.

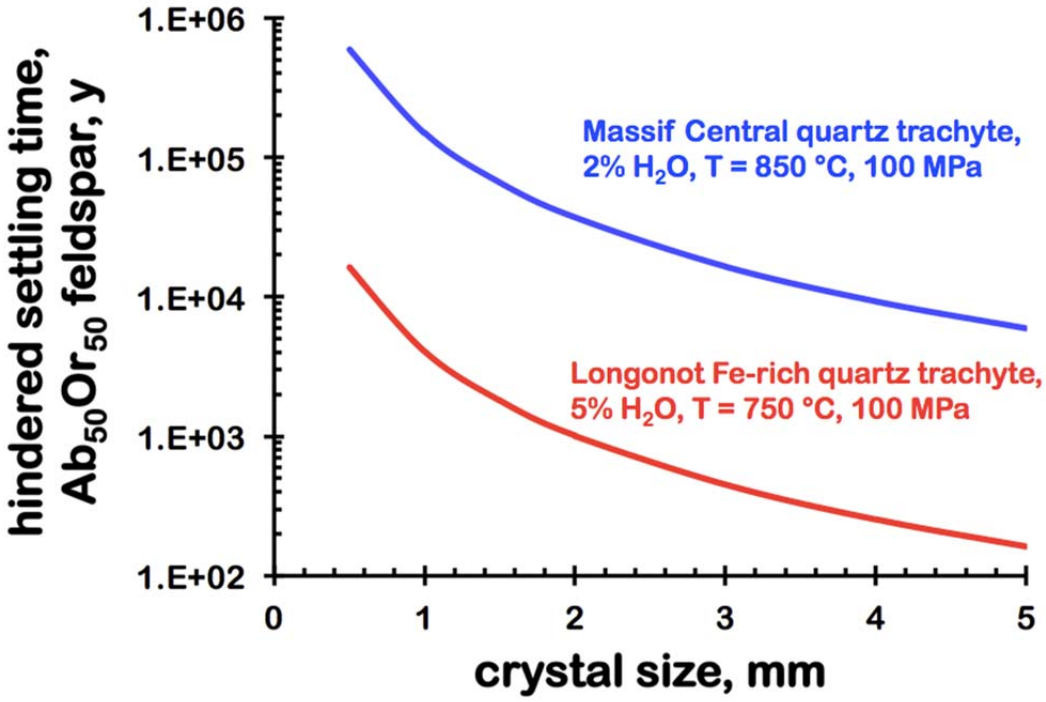

Figure DR4: Time for clarification of 500 m thickness of magma of initial crystallinity c = 0.3 by hindered settling of feldspar of composition $Ab_{50}Or_{50}$. The two examples shown encompass the range of results for the melt compositions in Table DR1. The minimum times are shorter than those calculated for granitoid systems by Bachmann and Bergantz (2004) by approximately half.

References in addition to those cited in the main paper:

Barnea, E., and Mizrahi, J., 1973, A generalized approach to the fluid dynamics of particulate systems. Part I. General correlation for fluidization and sedimentation in solid multiparticulate systems. Chemical Engineering Journal., v. 5, p. 171–189.

Ghiorso, M.S., and Sack, R.O., 1995, Chemical Mass Transfer in Magmatic Processes. IV. A Revised and Internally Consistent Thermodynamic Model for the Interpolation and Extrapolation of Liquid-Solid Equilibria in Magmatic Systems at Elevated Temperatures and Pressures: Contributions to Mineralogy and Petrology, v. 119, p. 197-212.

Giordano, D., Russell, J.K., and Dingwell, D.B., 2008, Viscosity of magmatic liquids: a model. Earth and Planetary Science Letters, v. 271, p. 123–134.

Gualda, G.A.R., Ghiorso, M.S., Lemons, R.V., and Carley, T.L., 2012, Rhyolite-MELTS: a modified calibration of MELTS optimized for silica-rich, fluid-bearing magmatic systems: Journal of Petrology, v. 53, p. 875-890.

Kress, V.C., and Carmichael., I.S.E., 1991, The compressibility of silicate liquids containing Fe_2O_3 and the effect of composition, temperature, oxygen fugacity and pressure on their redox state: Contributions to Mineralogy and Petrology, v. 108, p. 82–92.

Lange, R.A., and Carmichael, I.S.E., 1987, Densities of Na_2O-K_2O-CaO-MgO-FeO-Fe_2O_3-Al_2O_3-TiO_2-SiO_2 liquids: new measurements and derived partial molar properties. Geochimica et Cosmochimica Acta, v. 51, p. 2931–2946.

Lange, R.A., and Carmichael, I.S.E., 1990, Thermodynamic properties of silicate liquids with emphasis on density, thermal expansion and compressibility: Reviews in Mineralogy, v. 24, p. 25-64.

Ochs, F.A. III, and Lange, R.A., (1999) The density of hydrous magmatic liquids: Science, v. 283, p. 1314–1317.

Olin, PH, 2007, Magma dynamics of the Diego Hernández Formation, Tenerife, Canary Islands. PhD thesis, Washington State University, USA, 416 p.

Rogers, N.W., Evans, P.J., Blake, S., Scott, S.C., and Hawkesworth, C.J., 2004, Rates and timescales of fractional crystallization from ^{238}U–^{230}Th–^{226}Ra disequilibria in trachyte lavas from Longonot volcano, Kenya: Journal of Petrology, v. 45, p. 1747–1776.

Sharp, Z.D., Helffrich, G.R., Bohlen, S.R., and Essene, E.J., 1989, The stability of sodalite in the system $NaAlSiO_4$–NaCl: Geochimica et Cosmochimica Acta, v. 53, p. 1943–1954.